Available online at www.sciencedirect.com
SCIENCE DIRECT®
Journal of Nuclear Materials 346 (2005) 244–252
journal of nuclear materials
www.elsevier.com/locate/jnucmat

Fission gas release in FBR MOX fuel irradiated to high burnup

Koji Maeda *, Kozo Katsuyama, Takeo Asaga

Fuels and Materials Division, O-arai Engineering Center, Japan Nuclear Cycle Development Institute, 4002, Narita, O-arai-machi, Ibaraki 311-1393, Japan

Received 3 June 2004; accepted 19 June 2005

Abstract

Fission gas release in FBR MOX fuel pins irradiated to high burnup was studied as a function of burnup. Fuel pellets of different microstructures were fabricated by three methods. The pin averaged burnup of fuel pins ranged from 5.8 to 144 MWd/kgM. The fission gas release mechanism was investigated from results of the puncture test, microstructure observations and EPMA analyses. The fission gas release increased with the increase of burnup. But it depended on the microstructure of as-fabricated fuel below a burnup of 70 MWd/kgM. The difference in fission gas release among fuel pellets of different microstructures, could be attributed to fission gas which was retained in the large size pores of the as-fabricated fuel. In the fuel pin irradiated beyond burnup of 100 MWd/kgM, the fission gas release fraction was significantly large (nearly 80%), and independent of the burnup, the kinds of pellets and LHR. This indicated that little capacity for retention of fission gas is expected in the fuel irradiated to the burnup beyond 100 MWd/kgM and this should be considered in the FBR fuel pin design.

PACS: 28.41.Bm

1. Introduction

Fission gas release is of importance to fuel behavior for several reasons. The fission gases released from the fuel to the fuel-cladding gap increase the internal pressure and fuel temperature by degrading the thermal conductivity of the filled gas due to the mixing of heavy gas atoms in the gap. The fission gases which remain in the fuel form fission gas bubbles on both intra-granular and inter-granular regions, resulting in fuel swelling.

The basic mechanism of fission gas release is as follows [1,2]. A part of the fission gas generated in a fuel grain migrates to the grain boundary, and accumulates and forms fission gas bubbles there. With the increase of burnup, the bubbles grow by the continuous accumulation of fission gases from the intra-granular region by their coalescence with other bubbles. As a result, fission gas bubble tunnels, which interlink to the fuel surfaces, form on the grain-boundary and fission gas is released through them.

Recently, studies on fission gas release in LWR fuels have made great progress. In particular, fission gas release in fuel irradiated to high burnup has been investigated to extend the burnup [3]. It has been learned that the fission gas release increased with the increase of burnup and a restructuring to fine grains occurred on the pellet rim [4–6]. There are, however, few studies on fission gas release in FBR MOX fuel [7].

* Corresponding author. Tel.: +81 29 267 4141; fax: +81 29 267 7130.
E-mail address: k-mae@oec.jnc.go.jp (K. Maeda).

0022-3115/$ - see front matter © 2005 Elsevier B.V. All rights reserved.
doi:10.1016/j.jnucmat.2005.06.014

In this study, the fission gas releases were measured in 98 FBR MOX fuel pins taken from 18 fuel assemblies irradiated to 5–144 MWd/kgM in the experimental fast reactor, 'JOYO'. For some fuel pins, the concentration of Xe which remained in the fuel matrix was evaluated with EPMA (electron probe micro analyzer), and microstructural observations were made with an optical microscope and SEM (scanning electron microscope). The results were discussed, focusing on the burnup dependency.

2. Experimental method

2.1. Specimens and irradiation conditions

Three kinds of fuel pellets, pellet-1, pellet-2 and pellet-3, were fabricated from combinations of two types of powders and a pore former by conventional powder technology. The first powder was prepared by mixing UO_2 (ADU) powder and PuO_2 powder which were obtained by calcinating the oxalate. The second powder was a mixture of UO_2 (ADU) powder and MOX (mixed oxide) powder which was prepared by co-converting the mixed nitrate (Pu:U = 20:1) by microwave heating (MH) [8,9].

Pellet-1 was fabricated from the first powder without adding pore former. Whereas pellet-2 was fabricated from the second powder by adding pore former, because the second powder was highly sinterable. Pellet-3 was fabricated from the first powder by adding a significant amount of pore former.

The O/M ratio of fuel pellets was 1.98. The fissile content in the fuel was adjusted to nearly 31% by changing the content of ^{235}U, because the fissile content in PuO_2 depends on the raw powder supplied for the mixing. The fuel pellets were inserted into the cladding tubes of 20% cold worked PNC-316 along with insulator pellets, spring, etc. The length of the fissile column was 550 mm. After spacer wires were spirally wrapped around the fuel pins, they were assembled and inserted into a wrapper tube.

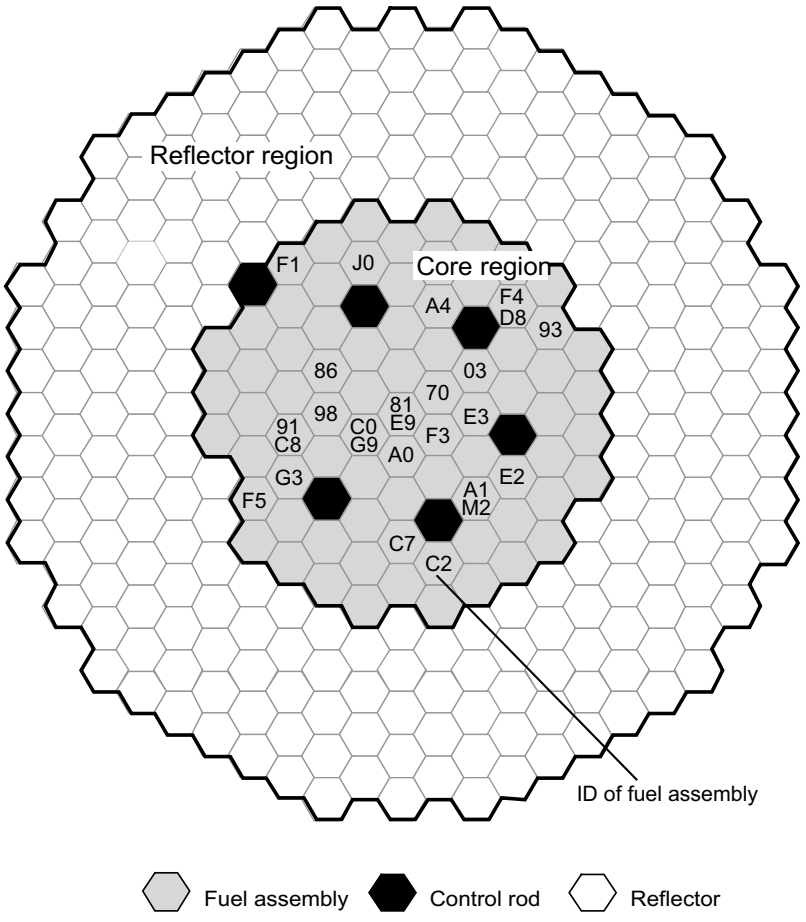

Fig. 1. Fuel assemblies and reflectors in JOYO MK-II core.

The configuration of the JOYO MK-II core is shown in Fig. 1. The core is comprised of fuel assemblies, control rods and surrounding reflectors. The designation of examined fuel assemblies and their initial loading positions are also shown in the figure. Fuel assemblies were shuffled from an inner position to an outer one, depending on operating requirements. The four kinds of fuel assemblies have their fuel pins arranged as shown in Fig. 2. The 'Driver' is the core fuel assembly. 'A', 'B' and 'C' signify the other fuel assembly types used for irradiation tests. Table 1 lists typical specifications and irradiation conditions of fuel assemblies used in this study.

From each fuel assembly, 5–10 fuel pins were taken out and subjected to the puncture test. One or two fuel pins among these ones were sectioned and subjected to other destructive examinations. The last two columns show the pin averaged burnup and linear heat rate (LHR), which were the largest in each fuel assembly.

2.2. Post irradiation examination

The amount of fission gas released from the fuel pellet to the free volume of a fuel pin was measured by the puncture test using a YAG (Yttrium Aluminum Garnet) laser. The Xe/Kr ratio was also measured by gas chromatography.

More than three segments were sectioned from one or two fuel pins in each fuel assembly. These segments were vacuum impregnated with epoxy resin and cut transversely into about 5 mm thick specimens. The transverse specimens were glued to epoxy stubs, and then ground and finally mirror polished. The fuel cross-sections thus obtained were examined by optical microscopy. In addition, the microstructural change, which occurred in the rim region of pellet, was observed with SEM.

2.3. Analysis of Xe by EPMA

The major gaseous fission product xenon is either present as dissolved atoms in the fuel matrix or as gas in pores. Quantitative analysis with EPMA was applied to the determination of the radial distribution of the Xe concentration in the fuel matrix. The analysis was carried out at an acceleration voltage of 25 kV and beam current of 1 μA. Under these conditions, the depth of electron beam penetration from the surface of a specimen would be about 0.5 μm and the region of X-ray excitation would be about 50 μm in diameter [10,11]. Due to the shallow depth of beam penetration, the amount of xenon measured by EPMA is not truly representative of total xenon retained in the fuel pellet. In this study, xenon retained in the fuel grains and precipitated in closed pores within a diameter of 0.1 μm is referred to as xenon retained in the fuel matrix, since EPMA has less sensitivity to detect xenon precipitated in bubbles larger than 0.1 μm [10].

Xenon retained in fuel matrix was investigated for dependence on burnup in terms of the amount of generated xenon, which was calculated by using the ORIGEN-2 code [12] after calculating the neutron

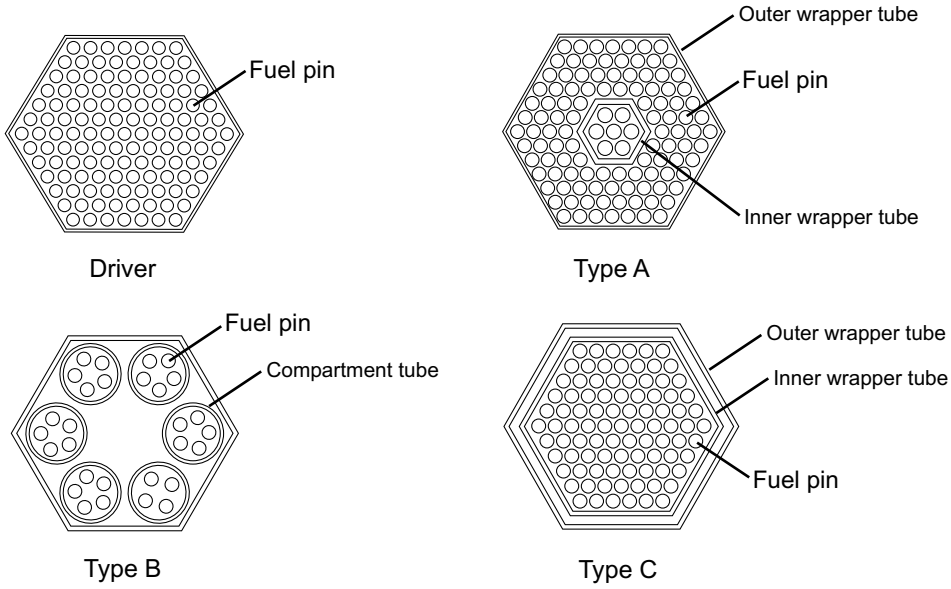

Fig. 2. Cross-sectional views of various fuel assemblies.

Table 1
Typical specifications and irradiation conditions of fuel assembly

Pellet type	PuO_2 powder	Fuel assembly designation	Type of fuel assembly	Fuel density %TD	Fuel diameter mm	Gap width μm	Pu spot size μm	Pore former w/o	Pin averaged	
									Burnup MWd/kgM	LHR kW/m
Pellet-1	Pu oxalate	81	Driver	93	4.63	160	90	–	37.7	26.1
		70	Driver	93	4.63	160	60	–	16.9	30.4
		03	Driver	93	4.63	160	<30	–	5.8	31.6
		86	Driver	93	4.63	160	<30	–	50.7	25.5
		91	Driver	93	4.63	160	90	–	56.0	30.9
		F4	Driver	93	4.63	160	50	–	39.8	26.4
		93	Driver	94	4.63	160	50	–	47.9	24.8
		C0	Driver	94	4.63	160	50	–	50.9	21.9
		A0	Driver	94	4.63	160	<30	–	59.6	26.1
		E3	Driver	94	4.63	160	0	–	69.6	32.0
		E2	Driver	94	4.63	160	<30	–	78.0	24.4
		E9	Driver	94	4.63	160	55	–	71.1	32.6
		F5	Driver	94	4.63	160	55	–	70.2	18.4
		M2	C	92	5.42	230	0	–	143.9	31.2
Pellet-2	Co-conversion Pu:U = 20:1	F3	Driver	94	4.63	160	60	0.3–0.8	60.6	32.6
		G9	Driver	94	4.63	160	<30	0.3–0.8	51.5	32.6
		C8	Driver	94	4.63	160	<30	0.3–0.8	81.3	32.0
		F1	Driver	94	4.63	160	<30	0.3–0.8	66.4	41.1
		C7	Driver	94	4.63	160	<30	0.3–0.8	70.5	30.5
		C2	Driver	94	4.63	160	<30	0.3–0.8	53.4	20.7
		J0	Driver	94	4.63	160	<30	0.3–0.8	71.3	20.0
		D8	Driver	94	4.63	160	138	0.3–0.8	57.5	20.4
		98	A	85	5.40	190	0	1.8	41.1	41.0
Pellet-3	Pu oxalate	A1	B	85	5.40	190	<40	1.3–1.5	56.5	30.2
		A4	C	85	5.40	190	<60	1.9	64.2	29.0
		G3	C	85	5.40	190	<60	1.9	119.2	27.2

cross-sections in the JOYO reactor core by the fast reactor group constant set, JFS-3-J3.2R [13]. Radial concentration profiles were obtained by point analysis at intervals of 50 μm. Calibration of xenon measurements was done using the outermost part of low burnup fuel specimens (below 20 MWd/kgM). Fission gases in this region were assumed to be completely retained at their generated position because of the low temperature.

3. Results and discussion

3.1. Microstructure of as-fabricated pellets

Fig. 3 shows the microstructures of the three kinds of as-fabricated fuel pellets. A few large pores can be seen in the microstructure of fuel pellet-1 fabricated from the first powder without the pore former, but there are a considerable number of pores in the microstructure of fuel pellet-2 fabricated from the second powder with pore former. In addition, a large number of big pores can be observed in the microstructure of the low-density pellet-3 (TD = 85%) fabricated from the first powder with the pore former.

3.2. Fission gas release by the puncture test

Amount of Xe retained in fuel was investigated as a function of burnup. Fig. 4 shows the amount of fission gas released from the fuel pellet to the pin free volume as a function of burnup. The total amount of fission gas generated in fuel was calculated by the ORIGEN-2 code and is shown as a straight line. The measured data are identified by pellet type (history of fabrication) and LHR range in order to clarify the effects of the history of pellet fabrication and LHR on the fission gas release.

Fraction of fission gas release was derived as the ratio of fission gas amount measured by puncture test to the total amount of generated Xe. Fig. 5 was drawn to show the dependence of fractional release of fission gas on the burnup. Details of burnup measurements have been reported in another paper [14].

In pellet-1 fabricated using the PuO_2 powder prepared from oxalate, a significant fission gas release begins at around 20 MWd/kgM and its amount increases with the increase of burnup and depends little on the LHR. On the other hand, in pellet-2 fabricated using the MOX powder prepared by the MH method, the fission gas release begins at around 40 MWd/kgM and

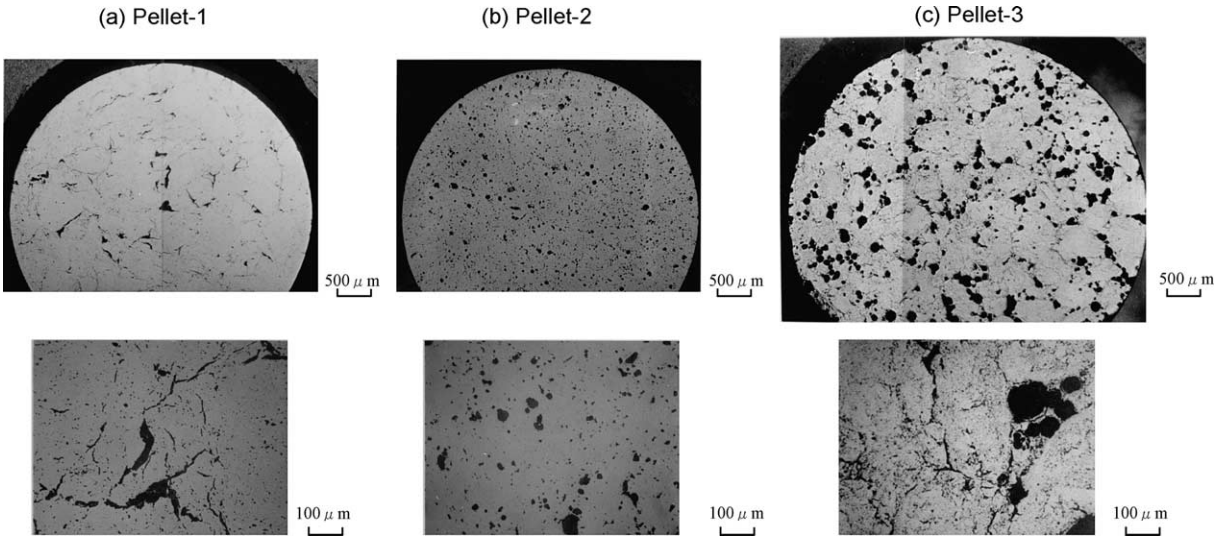

Fig. 3. Microstructure of the pellets fabricated by three different methods: (a) pellet-1: mixing of PuO_2 and ADU powders, (b) pellet-2: mixing of MOX powder (Pu:U = 20:1) and ADU powder, and adding pore former, (c) pellet-3: mixing of PuO_2 and ADU powders, and adding pore former.

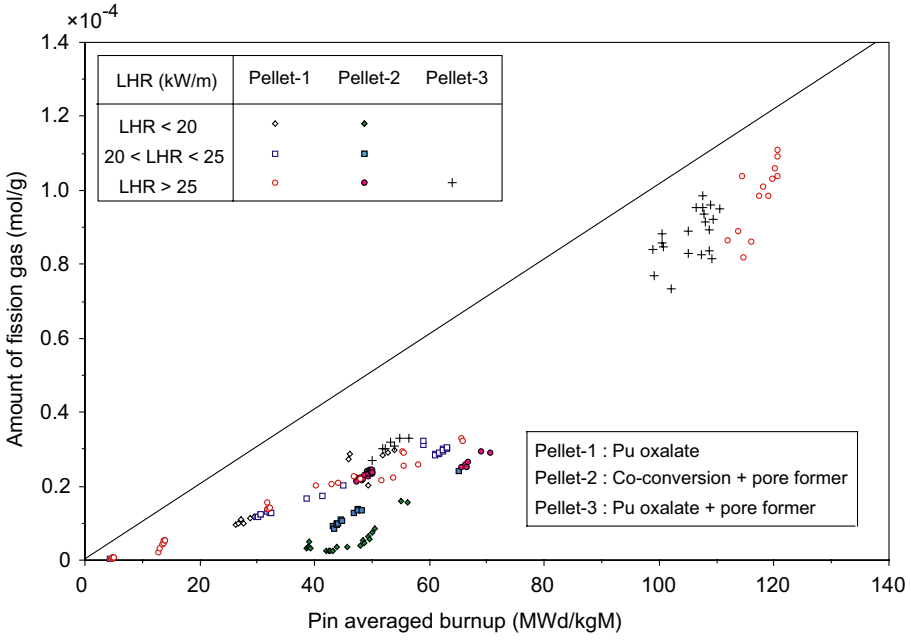

Fig. 4. The fission gas release measured by puncture test as a function of pin averaged burnup.

depends on the LHR. The difference in fission gas release between pellet-1 and pellet-2 can be explained as follows.

Generally, the fission gas generated in the fuel matrix migrates to a grain-boundary by the diffusion-trapping model [15], and then forms fission gas bubbles. As the amount of burnup increases, the bubbles coalescence with each other and subsequently form fission gas tunnels interlinked to the pellet surface. Finally the fission gas is released into the pin free volume. This mechanism suggests that the fission gas tunnels form at around 20 MWd/kgM in pellet-1.

Comparison of the microstructures between pellet-1 and pellet-2 shows there are a number of voids in

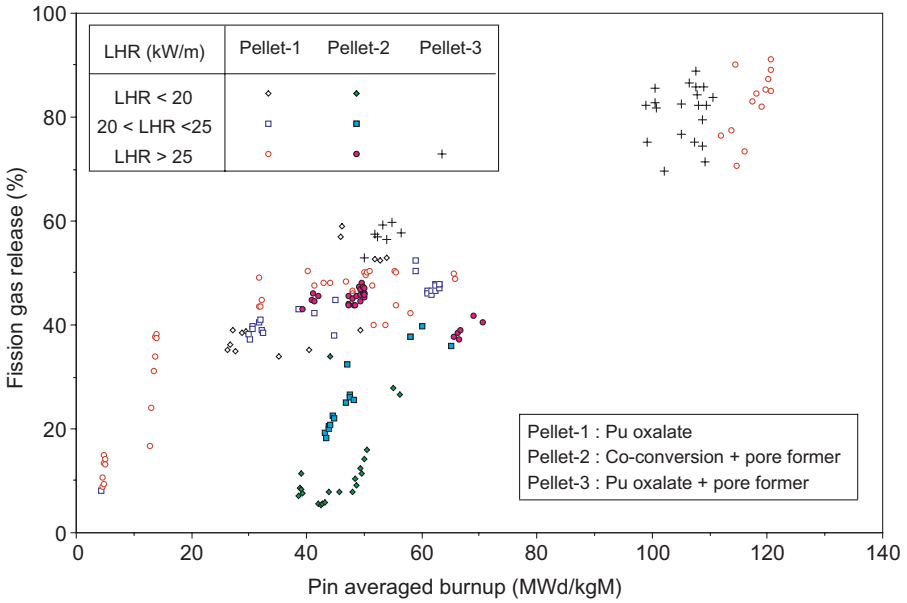

Fig. 5. Fractional release of fission gas as a function of pin averaged burnup.

pellet-2 (Fig. 3(b)) which was fabricated after doping with the pore former. These pore former voids have a retention capacity for fission gas in addition to the fission gas bubbles formed on the grain-boundary. Thus, the existence of these pore former voids shifts the beginning of fission gas release from ~20 to ~40 MWd/kgM. However, the pore former voids in pellet-2 were annihilated with the increase of LHR by fuel restructuring as shown in Fig. 6 and the fission gas accumulated there was released. For this reason, the fission gas release in pellet-2 increases with the increase of LHR.

As indicated in Fig. 5, the fission gas release fraction is higher in pellet-3 than in the other two pellets. Pellet-3 was fabricated by doping a large amount of pore former to lower its density (85%TD). It is, therefore, most likely that pellet-3 experienced high temperature during irradiation and this resulted in a large fission gas release fraction, since the thermal conductivity of fuel decreases with the decrease of fuel density.

In the pellets irradiated beyond ~100 MWd/kgM, the amount of fission gas release is significantly large, and independent of the kinds of pellets and LHR. Fig. 5 shows the fractional fission gas release is around 80%. As mentioned above, the bubbles of fission gas interconnect with each other on the grain-boundary after migration from the fuel matrix and subsequently form the tunnels leading to the fission gas release. With increasing burnup, these processes are repeated. The observations from Fig. 5 suggest that the retaining

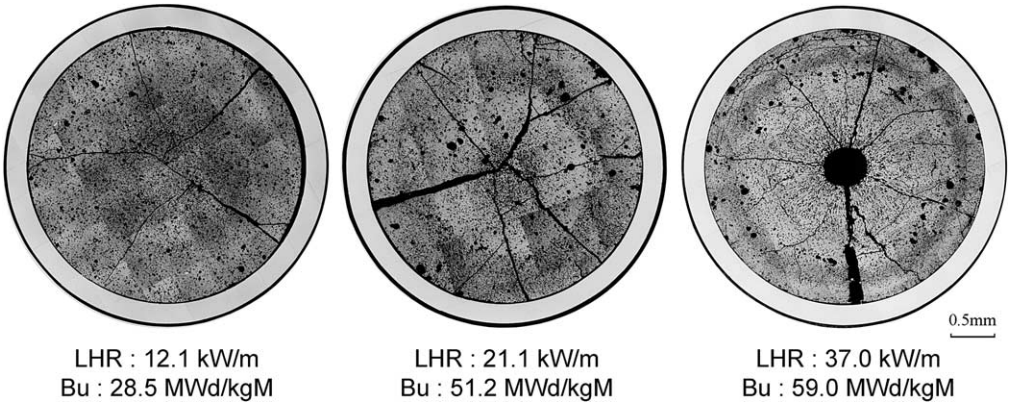

Fig. 6. Ceramographs of a restructured fuel in pellet-2 irradiated at different linear heat rate.

capacity of fission gas in the fuel is limited, and all fission gases generated beyond this capacity (~70 MWd/kgM) are released into the pin free volume.

3.3. Results by EPMA

It is important to know where the fission gas is retained in the irradiated fuel. Fig. 7 shows microstructures in a high burnup fuel pin (G3) obtained in cross-sections at three different axial positions, $x/L = 0.07$, 0.51 and 0.97, where L is total length of the fissile column and x is the distance from the bottom of that column. Fig. 8 shows the radial Xe concentration distributions measured on these cross-sections where the concentration (c/c_0) of Xe was defined as the ratio of the measured concentration (c) to the generated one (c_0) calculated by ORIGEN-2. Considerable concentrations of Xe are observed in both the lowest and highest axial positions ($x/L = 0.07$ and 0.97) at low surface temperature below 700 °C. But the concentration in the former axial position decreases with the increase of relative radius (r/R) in the rim region of the pellet.

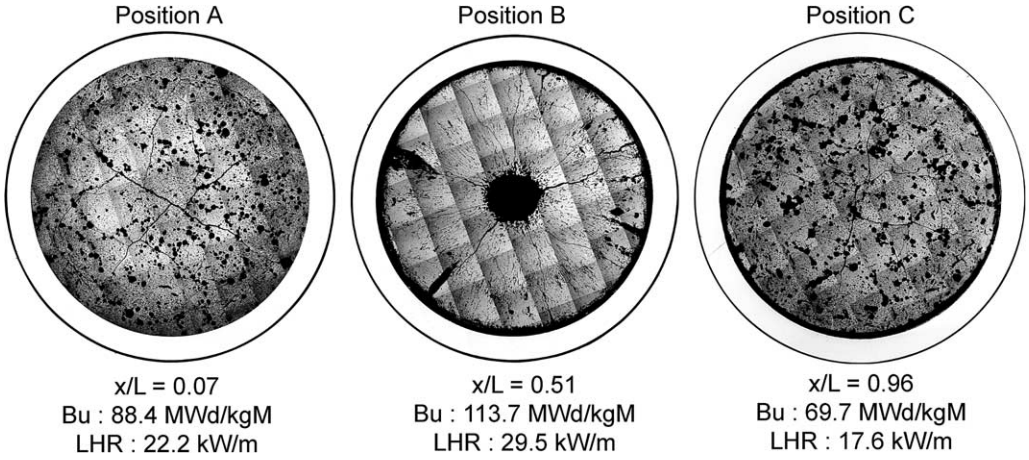

Fig. 7. Ceramographs of a representative high burnup fuel pin obtained at three transverse sections (G3 fuel pin, Pin Ave. burnup: 98.8 MWd/kgM).

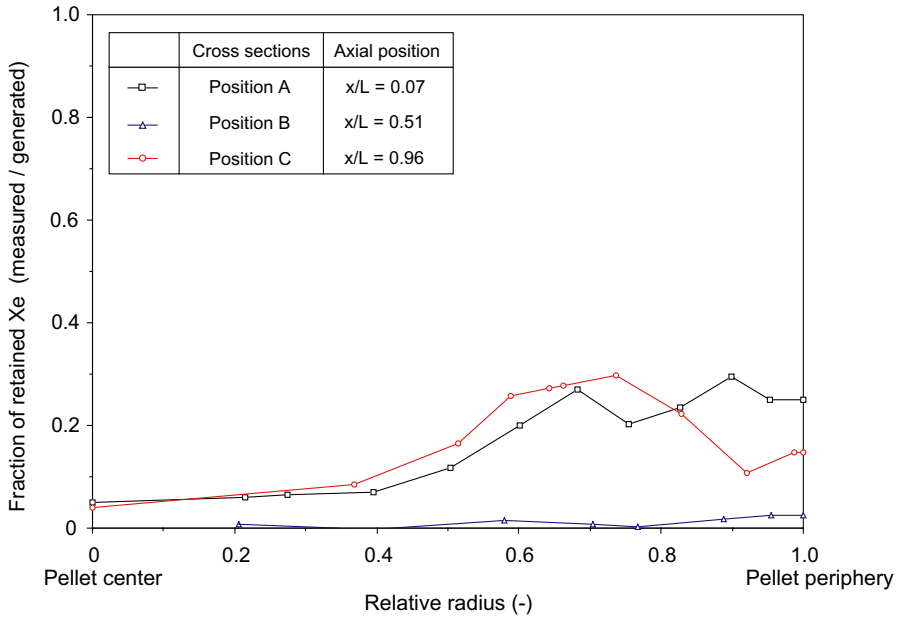

Fig. 8. Xe radial distributions measured on three cross-sections of a high burnup fuel pin (G3 fuel pin, Pin Ave. burnup: 98.8 MWd/kgM).

In the central position ($x/L = 0.51$) at high temperature, concentration is small ($c/c_0 < \sim 0.04$) in the whole radial region. From this low concentration near the outer surface of the pellet, Xe diffusion coefficient was tentatively derived, using the grain size and irradiation conditions of LHR and EFPDs (effective full power days). Based on Booth's model [1], the fractional release (f) could be expressed by the following equation:

$$f = 1 - \frac{6a^2}{90D^*_{Xe}t} + \frac{6a^2}{90D^*_{Xe}t}\sum_{n=1}^{\infty}\frac{1}{n^2}\exp\left(-\frac{n^2\pi^2 D^*_{Xe}t}{a^2}\right), \quad (1)$$

where D^*_{Xe} is the apparent diffusion coefficient of Xe, t is the time, and a is the radius of a grain. The radius a was assumed to be 5 μm from the microstructure of the fuel pellet before irradiation and the time t was 7.2×10^7 s from EFPD (833 days). In addition, the temperature near the outer surface of the pellet was 1000 °C. According to Matzke [16], D^*_{Xe} was expected to be less than 10^{-16} cm^2/s. Thus, the conditions, $f > 0.57$ and $D^*_{Xe}t/a^2 \leq 1$, would be in effect in Eq. (1) and the following approximation could be applied.

$$f = 4\frac{\sqrt{D^*_{Xe}t}}{\pi a^2} - \frac{3D^*_{Xe}t}{2a^2}. \quad (2)$$

For $f = 0.96$, $a = 5 \times 10^{-4}$ cm and $t = 7.2 \times 10^7$ s as described above, the solution $D^*_{Xe} = 2.6 \times 10^{-17}$ cm^2/s was obtained at ~850 °C of fuel surface temperature and 2.5×10^{13} fissions/s cm^3 of fission rate. The estimated diffusion coefficient could be compared with the controlled measurements, such as the ones reviewed by Matzke [16]. The corresponding irradiation enhanced diffusion coefficients was about one order of magnitude smaller than those for intrinsic self-diffusion of U and Pu in UO_2 and $(U,Pu)O_2$. In addition, compared with data of the enhanced in-pile release of fission gas reported by Friskney et al. [17], this estimated value shows a reasonable agreement.

Next, it is interesting to relate the EPMA results with the microstructures. At the central position, $x/L = 0.51$, where the LHR and fuel temperature are high, a typical restructuring along the steep temperature gradient can be seen in the microstructure. As a result, most of the fission gases are released.

In the microstructure of the lowest position at low temperature, $x/L = 0.07$, the restructuring is observed in the region $r/R > 0.7$. This is known as the high burnup structure [18]. And it can be typically seen in the rim of LWR fuel irradiated to high burnup [19]. In this region, the fuel temperature is low and then the capacity to retain fission gases is large in comparison with that of the central position, as shown in the EPMA results. Of interest is the microstructure at the highest position, $x/L = 0.97$ where the fuel temperature is intermediate. That is, the microstructure in the rim region $0.9 < r/R < 1.0$ varies, depending on the radial angle. In part of the rim region, the restructuring to fine grains is seen, but in another part, a white layer structure is observed around the outer surface of the pellet, which seems to be evolved from annihilation of fine grains in the rim region. Considering the decrease of Xe concentration toward the outer surface of the pellet shown in Fig. 8, it is suggested that part of the fission gases are released in this region.

4. Summary and conclusions

Fission gas release behavior was studied as a function of burnup in a large number of FBR MOX fuel pins irradiated to high burnup. Below the burnup of 70 MWd/kgM, the fission gas release increased with the increase of burnup, but the release depended on the microstructure of as-fabricated fuel.

In the fuel of high density (pellet-1) which was fabricated without pore former, the fission gas release began at about 20 MWd/kgM. Release began at about 40 MWd/kgM and depended on the LHR in the fuel of high density (pellet-2) which had many large size pores introduced by doping with pore former. The difference between the fission gas releases in both fuels could be explained by the retaining capacity of fission gas in the fuel. That is, a large amount of fission gas could be retained in large pores in addition to the intra-granular and inter-granular structures of the fuel, and then the beginning of fission gas release shifted to high burnup. Furthermore, the dependence of fission gas on the LHR could be suspected from the fact that large size pores disappeared through restructuring of fuel during irradiation.

In pellet-1 and pellet-3, which were irradiated beyond 100 MWd/kgM, the amount of fission gas release was significantly large, independent of the kinds of pellets and LHR. Nearly 80% of the fission gas generated was released from the fuel pellet to the pin free volume. From this fact, the capacity for retention of fission gas is not expected in fuel irradiated to burnups beyond 100 MWd/kgM.

Acknowledgements

The authors gratefully acknowledge very helpful discussions with Dr Hirotaka Furuya, Professor Emeritus, Kyushu University.

References

[1] A.H. Booth, A method for calculating fission gas diffusion from UO_2 and its application to the X-2-f loop test/Atomic

Energy of Canada Ltd., Chalk River, Ontario, Canada, Report AECL-496 (1957).
[2] R.J. White, M.O. Tucker, J. Nucl. Mater. 118 (1983) 1.
[3] R. Manzel, C.T. Walker, J. Nucl. Mater. 301 (2002) 170.
[4] K. Une, K. Nogita, T. Hosokawa, Y. Suzawa, S. Shimizu, Y. Etoh, J. Nucl. Mater. 278 (2000) 54.
[5] K. Une, K. Nogita, T. Shiratori, K. Hayashi, J. Nucl. Mater. 288 (2001) 20.
[6] C.T. Walker, J. Nucl. Mater. 275 (1999) 56.
[7] M. Tourasse, M. Boidron, B. Pasquet, J. Nucl. Mater. 188 (1992) 49.
[8] M. Koizumi, K. Ohtsuka, H. Isagawa, H. Akiyama, A. Todokoro, Nucl. Technol. 61 (1983) 55.
[9] M. Koizumi, K. Ohtsuka, H. Ohshima, H. Isagawa, H. Akiyama, A. Todokoro, K. Naruki, J. Nucl. Sci. Technol. 20 (7) (1983) 529.
[10] C. Ronchi, C.T. Walker, J. Phys. D13 (1980) 2175.
[11] C. Ronchi, Hj. Matzke, Fuel and Fuel Elements for Fast Reactors, IAEA, Vienna, 1974, p. 57.
[12] A.G. Croff, ORNL-5621 (1980).
[13] G. Chiba, T. Hazama, M. Ishikawa, Trans. At. Energy Soc. Jpn. 1 (4) (2002) 335 (in Japanese).
[14] S. Koyama, M. Osaka, T. Sekine, K. Morozumi, T. Namekawa, M. Itoh, J. Nucl. Sci. Technol. 40 (12) (2003) 998.
[15] D. Olander, Fundamental Aspects of Nuclear Reactor Fuel Elements, TID26711-P1 (1976).
[16] Hj. Matzke, Radiat. Eff. 53 (1980) 219.
[17] C.A. Friskney, J.A. Turnbull, J. Nucl. Mater. 79 (1979) 184.
[18] K. Lassmann, C.T. Walker, J. van de Laar, F. Lindstrom, J. Nucl. Mater. 226 (1995) 1.
[19] M. Mogensen, J.H. Pearce, C.T. Walker, J. Nucl. Mater. 264 (1999) 99.